Simulating the Respect of a Functional Condition in a Mechanical System with Mobilities

Denis Teissandier, Vincent Delos, Sonia García

Available online at www.sciencedirect.com

ScienceDirect

Procedia CIRP 00 (2019) 000–000

www.elsevier.com/locate/procedia

CIRP CAT 2020

Simulating the Respect of a Functional Condition in a Mechanical System with Mobilities

Denis Teissandier[a], Vincent Delos[b], Sonia C. García[a,*]

[a] *Univ. Bordeaux, I2M, UMR 5295, F-33400 Talence, France*
[b] *CNRS, I2M, UMR 5295, F-33400 Talence, France*

Abstract

Geometric tolerance analysis with sets of constraints is an issue to address to model over-constrained architectures. This article is based on the implementation of sets of constraints with prismatic polyhedra. The conformity of a mechanical system with respect to a functional condition is formalized by the inclusion of a resulting polyhedron in a functional polyhedron. After giving the definition of a functional condition, the general inclusion method is presented. An example illustrates the inclusion conditions.

Keywords: Tolerance analysis ; Sets of constraints ; Prismatic polyhedron ; Geometric algorithms

1. Introduction

Geometric tolerancing analysis of over-constrained mechanisms consists in closing contacts loops where degrees of freedom are suppressed in a redundant way. One of the means to achieve this goal is to use operations on sets of constraints (SOC). The latter can characterize not only the geometric variations but also the contacts.

These operations are the Minkowski sum and the intersection. A sum is required for the serial contact architectures while an intersection has to be performed for the parallel contact architectures. The reduction of a mechanical system architecture combining sums and intersections allows to determine the relative location between two faces of two parts in any mechanical system with the corresponding SOC. The inclusion of the resulting SOC in a functional SOC –modelling a functional requirement– simulates the conformity of a mechanical system [1].

Among the works realized in tolerancing analysis [2], the domains proposed by Giordano et al. and the T-Maps introduced by Davidson et al. can process simultaneously geometric variations of the parts and their contacts following this type of approach [3]. However, the applications are always performed in a subspace of the bounded displacements where the resulting SOC and the functional SOC are closed. Nevertheless, in general the functional requirement and the architecture of a mechanism will generate unbounded SOCs due to the degrees of freedom in a space of dimension 6.

This paper proposes the general formulation of the inclusion of a prismatic polyhedra (resulting SOC) in an other one (functional SOC) in dimension 6. This formulation remains valid if the SOC are polytopes.This paper shows how to describe and compute this inclusion with sets of constraints modelled by prismatic polyhedra. The prismatic polyhedra formalism allows to decompose a set of $\mathbb{R}^6$ operands (3 rotations, 3 translations) into a sum of a bounded set (a polytope) with straight lines. The polytope characterizes the limits of the bounded displacements, into an affine subspace whose dimension is lower than 6 [4].

These displacements are limited by part tolerances or joint clearance. The sum of the straight lines characterize the affine subspace generated by the surface invariance degree or the joint mobility degree. One of the difficulties in tolerancing is to differentiate the bounded displacements from the unbounded ones -which are theoretically unlimited [5]. The prismatic polyhedron integrates both bounded and unbounded displacements into the same model.

This work has been carried out under hypothesis of (i) infinitely rigid bodies, and (ii) the assumption that small displacements of nodes deriving from meshed surfaces can lead to lin-

* Corresponding author. Tel.: +33-7-69-00-51-23.
E-mail address: sonia.garcia-gomez@u-bordeaux.fr (Sonia C. García).

ear constraints. The first hypothesis means that the deformation of the constitutive parts of the mechanisms are not taken into account while the second one allows to model the dependencies between rotations and the translations as linear relations. The mesh of the toleranced features allows to generate linear boundaries, in order to manipulate only linear objects (polyhedra). Although T-maps and domain models are initially able to handle quadratic constraints [11, 12], the constraints are finally linearized because of the complexity of summing convex non-linear constraints in dimension 6.

2. Simulating variations with prismatic polyhedra

2.1. Characterizing an operand with a prismatic polyhedron

An operand SOC describes the displacement restrictions of a surface. This surface simulates the manufacturing defects relative to a nominal surface in a tolerance zone or the displacement restrictions between two surfaces potentially in contact (see Figure 1):

$$\forall N_i \in S_0, \forall i \in \{1, ..., m\} : d_{inf} \leq \mathbf{t}_{N_i}.\mathbf{n}_i \leq d_{sup} \quad (1)$$

The vector $\mathbf{t}_{N_i}$ is the translation of a point $\mathbf{N}_i$ belonging to the nominal surface S_0. It is possible to write this translation in a point M rigidly linked to the points N_i where $\mathbf{r}$ designates the rotation vector between the surfaces S_0 and S_1 according to small displacements hypothesis :

$$\forall i \in \{1, ..., m\} : d_{inf} \leq (\mathbf{t}_M + \mathbf{N}_i\mathbf{M} \times \mathbf{r}).\mathbf{n}_i \leq d_{sup} \quad (2)$$

After having defined in the basis (u, v, w) these vectors:

$$\begin{cases} \mathbf{r} = (r_u, r_v, r_w)^t \\ \mathbf{t}_M = (t_u, t_v, t_w)^t \\ \mathbf{N}_i\mathbf{M} = (d_{iu}, d_{iv}, d_{iw})^t \\ \mathbf{n}_i = (n_{iu}, n_{iv}, n_{iw})^t \end{cases}$$

We get the following relation:

$$\begin{aligned} d_{inf} \leq\ & (n_{iv}d_{iw} - n_{iw}d_{iv})x_1 + (n_{iw}d_{iu} - n_{iu}d_{iw})x_2 \\ & + (n_{iu}d_{iv} - n_{iv}d_{iu})x_3 + n_{iu}x_4 + n_{iv}x_5 + n_{iw}x_6 \leq d_{sup} \end{aligned} \quad (3)$$

with $x_1 = r_u, x_2 = r_v, x_3 = r_w, x_4 = t_u, x_5 = t_v, x_6 = t_w$, $\forall i \in \{1, ..., m\}$.

The relation 3 defines two $\mathbb{R}^6$ half-spaces. Intersecting all of them generates a $\mathbb{R}^6$ polyhedron such as:

$$\Gamma = \bigcap_{k=1}^{2m} \overline{H_k} \quad (4)$$

where, $\overline{H_k} = \left\{\mathbf{x} \in \mathbb{R}^6 : b_k + a_{k1}x_1 + ... + a_{k6}x_6 \geq 0\right\}$, $\forall k \in \{1, ..., 2m\}$.

The polyhedron Γ is bounded if the toleranced surface is classified as complex or if the contact between the two surfaces is a permanent connection where all the degrees of freedom are suppressed. In all the other cases, the polyhedron Γ is not bounded. Decomposing a polyhedron Γ in a sum of a polytope P and a polyhedral cone C is always possible -although not unique- according to the Minkowski-Weyl theorem [6] :

$$\Gamma = P \oplus C \quad \text{with } C = \sum_i \alpha_i \mathbf{a}_i,\ \alpha_i \geq 0,\ \mathbf{a}_i : \text{vector of } \mathbb{R}^n \quad (5)$$

A systematic decomposition of Γ in the sum of a polytope P and a polyhedral cone C has been proposed by Arroyave et al. [4]. The principle is to isolate the bounded displacements by the restrictions of a surface inside a zone (or between two surfaces potentially in contact) in the polytope P from the unbounded displacements in the polyhedral cone C. In the concept of screw [7] bounded and unbounded displacements belong to two orthogonal sub-spaces in the affine space.

The polyhedral cone C is a sum of linearly independent $\mathbb{R}^6$ straight lines Δ_j. Each line Δ_j is defined by its pluckerian coordinates: it is induced by a rotation mobility or a translation mobility to the point M rigidly linked to the points N_i generating the restrictions. The pluckerian coordinates of a straight line define a "twist screw" [7].

The hyperplane H_{Δ_j}, orthogonal to Δ_j, defines a "wrench screw" (forces and torques compliant with Δ_j mobility): it corresponds to the dual sub-space of the unbounded displacements, i.e. the bounded displacements sub-space. Finally we get:

$$\Gamma = \bigcap_{k=1}^{2m} \overline{H_k} = \left(\bigcap_{k=1}^{2m} \overline{H_k} \cap \left(\bigcap_j H_{\Delta j}\right)\right) + \sum_j \Delta_j = P + \sum_j \Delta_j \quad \text{with} \quad H_{\Delta j} \perp \Delta_j \quad (6)$$

For more details see [4] and [8].

2.2. Formulating a functional requirement

We consider the system depicted in Figure 2. This system is a sub-set of a sharpening device coming from a flexible material cutting machine –such as textile. A pulley 3 is in turning pair following the straight line $(C, \mathbf{z})$ with a mobile arm 2. This

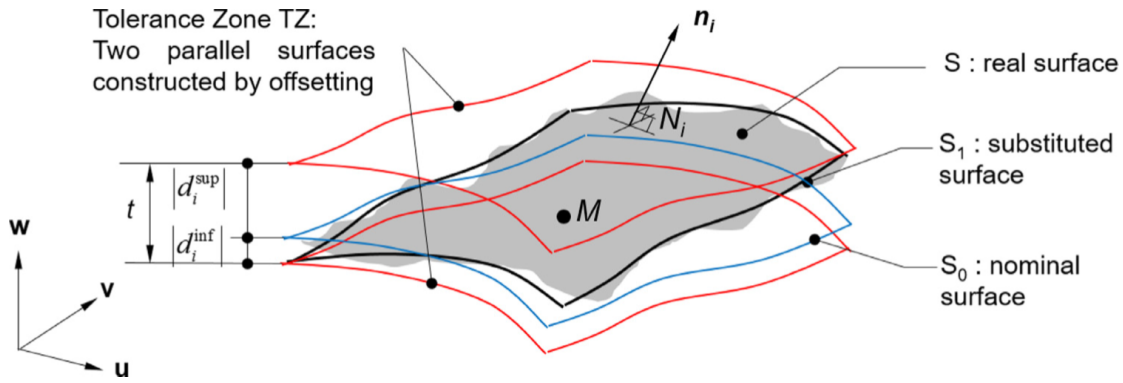

Fig. 1. Displacement restrictions of a surface in a tolerance zone [5].

joint results from the parallel association of two spherical pairs coming from the rolling bearings. To simplify the model, the level of details has been reduced. The mobile arm 2 is globally in prismatic pair with the tension arm 1 according to the line $(B, \mathbf{x})$. More precisely, this prismatic pair is a parallel combination of a cylindrical and a ball-and-plane pairs. The cylindrical pair according to the straight line $(B, \mathbf{x})$ is ensured by the couple of cylindrical surfaces 2,3 and 1,3. A no-headed screw linked to part 1 ensures a bilateral ball-and-plane pair at point A according the y-axis through the cylindrical surface 1,2 in contact with the sides of the groove 2,2.

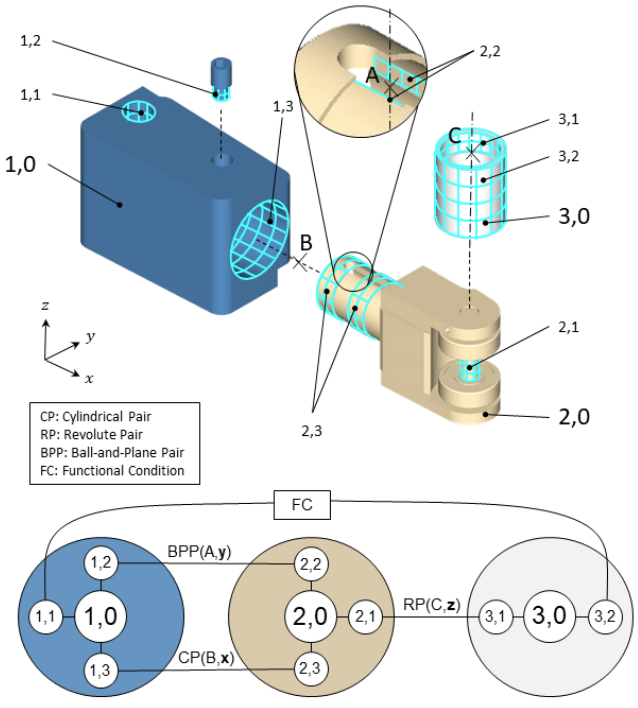

Fig. 2. The sharpening system.

The Functional Condition FC consists in controlling the parallelism between the external surface 3,2 from the pulley 3 and the cylindrical hole 1,1 from the tension arm 1. It is modelled as stated by the following method. The surfaces 1,1 and 3,2 are FC terminal surfaces. They are respectively included in two tolerance zones. These two zones are located and/or oriented between them according to internal mobilities. The two zones are two coaxial cylinders whose respective median cylinders are the nominal cylinders of the surfaces. These two zones have been assigned functional tolerances $t_{f_{1,1}}$ and $t_{f_{3,1}}$, see Figure 3. The prismatic polyhedron associated to the Functional Condition FC is defined by the relation 7 where the internal mobilities between the two zones are represented by a sum of straight lines:

$$\begin{aligned}\Gamma_f &= P_f \oplus \sum_w \Delta_w \\ &= \Gamma_{f_{1,1}} \oplus \Gamma_{f_{3,2}} \oplus \sum_c \Delta_c \\ &= \left(P_{f_{1,1}} \oplus \sum_u \Delta_u\right) \oplus \left(P_{f_{3,2}} \oplus \sum_v \Delta_v\right) \oplus \sum_c \Delta_c\end{aligned} \tag{7}$$

The prismatic polyhedron Γ_f is the Minkowski sum of the polyhedra coming from the terminal surfaces 1,1 and 3,2 and a sum of straight lines Δ_c. The polyhedra $\Gamma_{f_{1,1}}$ and $\Gamma_{f_{1,3}}$ are defined as two SOC operands according to (6). The straight lines Δ_c represent for the designer the mobilities that he wants to integrate or not into the Functional Condition. If the sharpening system is considered as a unique fictive part, then the sum of the lines Δ_c is the neutral element , that is to say the origin in the $\mathbb{R}^6$ space of displacements. The sub-space of unbounded displacements by FC does only depend on intrinsic mobilities to the terminal surfaces and to their relative locations in the sharpening system nominal model. This sub-space is defined by the sum of two unbounded displacements sub-spaces: $\sum_u \Delta_u + \sum_v \Delta_v$.

In our example where $\tau_{1,1}$ and $\tau_{3,1}$ are "twist screw" subspaces respectively associate to the terminal surfaces 1,1 and 3,1 at point M, we get (8):

$$\sum_u \Delta_u = \tau_{1,1} = \begin{bmatrix} \mathbf{z}, \mathbf{0} \\ \mathbf{0}, \mathbf{z} \end{bmatrix} = \begin{bmatrix} 0\,0\,1\,0\,0\,0 \\ 0\,0\,0\,0\,0\,1 \end{bmatrix}$$
$$\sum_v \Delta_v = \tau_{3,1} = \begin{bmatrix} \mathbf{z}, \mathbf{MN} \wedge \mathbf{z} \\ \mathbf{0}, \mathbf{z} \end{bmatrix} = \begin{bmatrix} 0\,0\,1\,0\,-L\,0 \\ 0\,0\,0\,0\,\;0\;\,1 \end{bmatrix}$$
$$\sum_u \Delta_u \oplus \sum_v \Delta_v = \tau_{1,1} \cup \tau_{3,1} = \begin{bmatrix} \mathbf{z}, \mathbf{0} \\ \mathbf{z}, \mathbf{MN} \wedge \mathbf{z} \\ \mathbf{0}, \mathbf{z} \end{bmatrix} = \begin{bmatrix} 0\,0\,1\,0\;\;0\;\;0 \\ 0\,0\,1\,0\,-L\,0 \\ 0\,0\,0\,0\;\;0\;\;1 \end{bmatrix} \tag{8}$$

In this case, FC is an orientation condition. Consequently, we have to add a translation mobility according to the x-axis between the two zones following the x direction. It finally comes to (9):

$$\sum_u \Delta_u \oplus \sum_v \Delta_v \oplus \sum_c \Delta_c = \tau_{1,1} \cup \tau_{3,1} \cup \tau_c = \begin{bmatrix} \mathbf{z}, \mathbf{0} \\ \mathbf{z}, \mathbf{MN} \wedge \mathbf{z} \\ \mathbf{0}, \mathbf{z} \\ \mathbf{0}, \mathbf{x} \end{bmatrix} = \begin{bmatrix} 0\,0\,1\,0\;\;0\;\;0 \\ 0\,0\,1\,0\,-L\,0 \\ 0\,0\,0\,0\;\;0\;\;1 \\ 0\,0\,0\,1\;\;0\;\;0 \end{bmatrix} \quad \text{with } \tau_c = [\mathbf{0}, \mathbf{x}] \tag{9}$$

Figure 3 shows graphically the projections of the polyhedra $\Gamma_f, \Gamma_{f_{1,1}}, \Gamma_{f_{3,1}}$ in the sub-spaces of the rotations (Figure 3b) and translations (Figure 3c). These polyedra derive from the CAD space (Figure 3a). The notation $\Pi()$ designates the orthogonal projection from the $\mathbb{R}^6$ displacement space to a $\mathbb{R}^3$ sub-space: the one of rotations or translations. Figure 3b illustrates the 2D sub-space of the bounded rotations (rotations according to x-axis and y-axis) and the 1D sub-space of the unbounded rotations (rotation according to z). Figure 3c shows the 0D sub-space of the bounded translations (the origin of the space) and the 3D sub-space of the unbounded translations.

2.3. *Simulating a system compliance with respect to a requirement*

Simulating a system compliance with respect to a requirement relies on three main steps. The first one consists in formulating SOC operands, this process has been previously described in the section 2.1.

The contacts allow to set up the relations between parts and can be formalized thanks to a graph. Such an example has been provided in section 2.2. Each edge from the graph is associated to a prismatic polyhedron. Computing the relative position between two surfaces in a mechanical system can be performed through a graph reduction. This reduction is the second step. It is based on summing serial edges and intersecting parallel edges and finally comes to a single edge connected to to the two main vertices. These vertices correspond to FC terminal surfaces. The algorithms summing and intersecting prismatic polyhedra are presented in [9] and [8].

Figure 4 depicts the graph reduction applied to the sharpening system. The 3D prismatic polyhedra in Figure 4 are 6D projections into the sub-space of the rotations according to the 3 directions x, y and z. This choice comes from the fact that the Functional Condition FC is an orientation condition, so we can visualize the polyhedra by projecting them from $\mathbb{R}^6$ into $\mathbb{R}^3$. The last step checks the inclusion of the polyhedron Γ_r resulting from the graph reduction into the target polyhedron Γ_f.

3. Formalizing the inclusion

Let Γ_r be the polyhedron resulting from the graph reduction. Let Γ_f be the target polyhedron modelling the Functional Condition FC. In a mechanical system, the geometric variations of the parts are compliant with FC if and only if :

$$\Gamma_r \subseteq \Gamma_f \quad \text{with} \quad \Gamma_r = P_r \oplus \sum_u \Delta_u \quad \text{and} \quad \Gamma_f = P_f \oplus \sum_v \Delta_v \tag{10}$$

Moreover we get:

$$\begin{aligned} P_r &= \bigcap_{k_r} \overline{H_{k_r}} \cap \left(\bigcap_u H_{\Delta u} \right), \text{with } H_{\Delta u} \perp \Delta_u \\ P_f &= \bigcap_{k_f} \overline{H_{k_f}} \cap \left(\bigcap_v H_{\Delta v} \right), \text{with } H_{\Delta v} \perp \Delta_v \end{aligned} \tag{11}$$

Checking the inclusion can be even more difficult if the bounded displacement sub-spaces coming from Γ_r and Γ_f are not the same.

So we consider the following property taking into account (10) and (11):

$$\sum_u \Delta_u \subseteq \sum_v \Delta_v \quad \text{and} \quad P_r \subseteq P_f \quad \Rightarrow \; \Gamma_r \subseteq \Gamma_f \tag{12}$$

We are going to check at first that Γ_r unbounded displacement sub-space is included into Γ_f unbounded displacement sub-space. In other words, we want to verify that the mobilities inherent to the architecture of the mechanical system are compliant with the Functional Condition. If it is not the case, satisfying equation (10) is impossible whatever tolerances and clearances are. It would happen if, for example, the ball-to-plane pair between the surfaces 1,2 and 2,2 disappeared (see Figures 2, 4 and 3 right). The rotation DOF between parts 1 and 2 according to the x-axis would prevent from controlling the parallelism between surfaces 1,1 and 3,2.

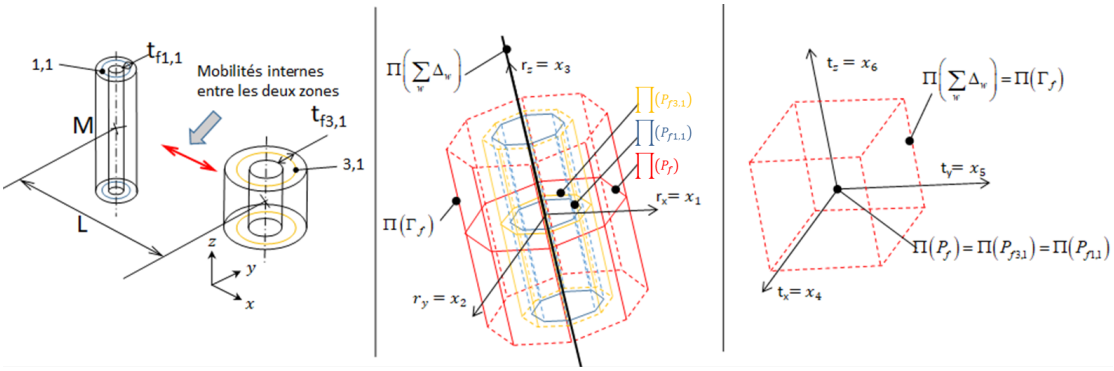

3a: CAD space

3b: Deviation space
rotation sub-space

3c: Deviation space
translation sub-space

Fig. 3. Modelling the Functional Condition FC.

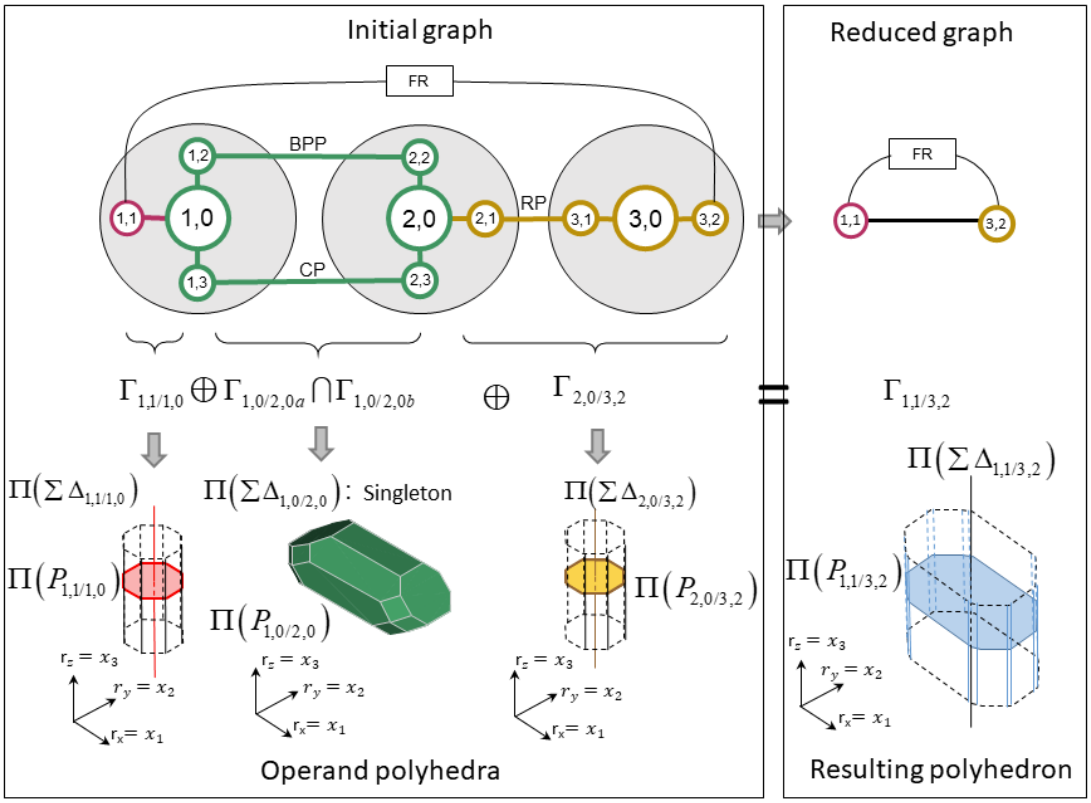

Fig. 4. The contact graph reduction.

$$\sum_u \Delta_u \subseteq \sum_v \Delta_v \Leftrightarrow \forall u : \Delta_u \perp \left(\bigcap_v H_{\Delta v}\right) \quad (13)$$

We want to use property 13 because it can check that the ubounded displacements space of Γ_r is orthogonal to the bounded displacements space of Γ_f.

From a mechanical point of view it means that any unbounded displacement (twist screw) of the prismatic polyhedron Γ_r generates a null power following the bounded displacements (wrench screw) of the prismatic polyhedron Γ_f. This is equivalent to computing the product of a twist screw and of a wrench screw that must be null.

Important remark: the property 13 can be satisfied only if

$$\dim\left(\sum_u \Delta_u\right) \leq \dim\left(\sum_v \Delta_v\right) \quad (14)$$

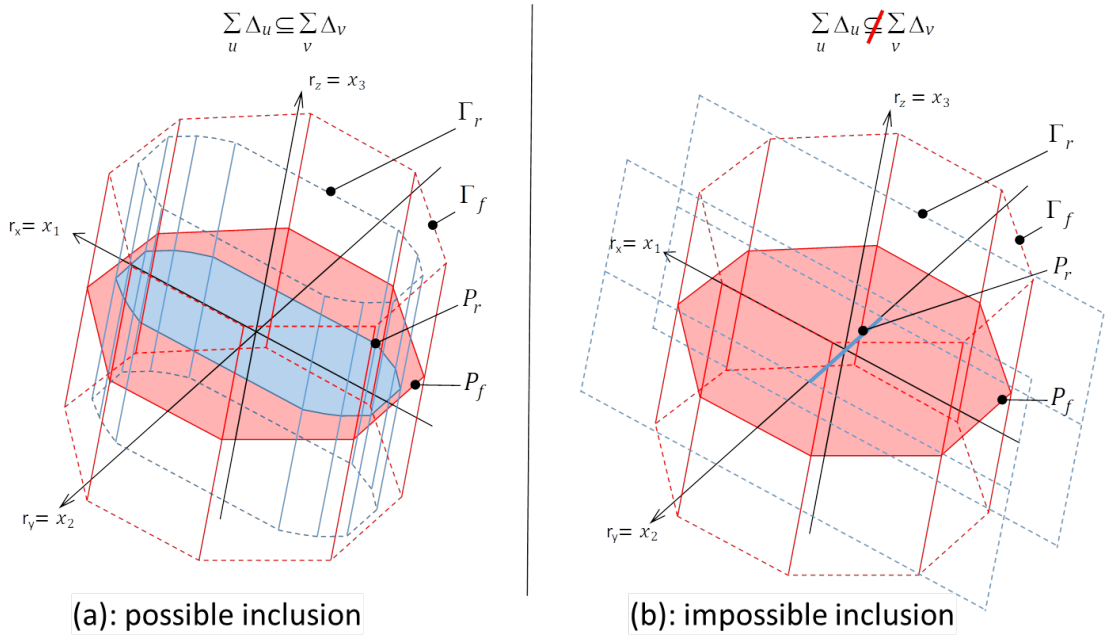

Fig. 5. Including the resulting polyhedron into the functional one.

If the relation 13 was verified (see Figures 3 left), including the polyhedron Γ_r into the polyhedron Γ_f only depends on including the polytope P_r into the polytope P_f. It can be easily done checking that all vertices of P_r are included into all the half-spaces defining Γ_f.

$$P_r \subseteq P_f \Leftrightarrow \forall v \in \mathcal{V}(P_r), \forall k_f : \quad v \in \overline{H_{kf}} \tag{15}$$

4. Conclusion

After having introduced the concept of a Functional Condition between two surfaces, this paper explains how to characterize the inclusion of a prismatic polyhedron into another one in $\mathbb{R}^6$ when their underlying polytopes do not share the same dimension. This method is especially interesting when checking the inclusion depends on a mobility of the system. If it is the case, it immediately concludes that satisfying the Functional Condition is impossible. If not, we can assess whether the filling of the functional polyhedron has been optimized or not. This opens the way to choosing better tolerances and clearances.

References

[1] S. Arroyave Tobon, D. Teissandier, V. Delos, Tolerance analysis with polytopes in HV-description, ASME J Comput Inf Sci Eng, DOI http://dx.doi.org/10.1115/1.4036558, 2017.
[2] Y. Cao, T. Liu, J. Yang, A comprehensive review of tolerance analysis models. The International Journal of Advanced Manufacturing Technology, 97/5–8: 3055–3085, 2018
[3] G. Ameta, S. Samper, M. Giordano, Comparison of Spatial Math Models for Tolerance Analysis: Tolerance-Maps, Deviation Domain, and TTRS. Journal of Computing and Information Science in Engineering 11(2), 2011.
[4] S. Arroyave Tobon, D. Teissandier, V. Delos, Applying screw theory for summing sets of constraints in geometric tolerancing, Mech. Mach. Theory, Vol. 112, pp. 255-271, 2017.
[5] L. Homri, D. Teissandier, A. Ballu, Tolerance analysis by polytopes: Taking into account degrees of freedom with cap half-spaces, Comput Aided Des, Vol. 62:112-130, 2015.
[6] G. M. Ziegler, Lectures on polytopes, Springer Verlag, 1995.
[7] J.D. Adams, Feature based analysis of selective limited motions in assemblies, MIT, Md thesis, 1998.
[8] S. Arroyave Tobon, Polyedral models reduction in geometric tolerance analysis, Phd thesis, Mecanique et Ingenierie, University of Bordeaux, 2017.
[9] V. Delos, D. Teissandier, S. Arroyave-Tobon, Introducing a Projection-Based Method to Compare Three Approaches Computing the Accumulation of Geometric Variations, ASME 2018 International Design Engineering Technical Conferences and Computers and Information in Engineering Conference, ASME, 2018, Quebec City
[10] D. Teissandier, V. Delos, PolitoCAT, Polytopes applied to Computer Aided Tolerancing, i2m.u-bordeaux.fr/politopix, 2016.
[11] M. Giordano, D. Duret, S. Tichadou, and R. Arrieux, Clearance Space in Volumic Dimensioning, CIRP Annals, vol. 41, no. 1, pp. 565–568, Jan. 1992.
[12] J. K. Davidson, A. Mujezinovic´, and J. J. Shah, A New Mathematical Model for Geometric Tolerances as Applied to Round Faces, J. Mech. Des, vol. 124, no. 4, pp. 609–622, Dec. 2002.